CONF-970201--33

final draft of paper presented at *Symposium on Fundamentals of Gamma Titanium Aluminides*, 1997 TMS Annual Meeting, Orlando, FL; for publication in **Metallurgical and Materials Transactions A**

DEVELOPMENT OF ULTRAFINE, LAMELLAR STRUCTURES IN TWO-PHASE γ-TiAl ALLOYS

P.J. Maziasz and C.T. Liu
Metals and Ceramics Division
Oak Ridge National Laboratory

ABSTRACT

Processing of two-phase γ-TiAl alloys (Ti-47Al-2Cr-2Nb or minor modifications thereof) above the α-transus temperature (T_α) produced unique refined-colony/ultrafine lamellar structures in both powder- and ingot-metallurgy (P/M and I/M, respectively) alloys. These ultrafine lamellar structures consist of fine laths of the γ and α_2 phases, with average interlamellar spacings (λ_L) of 100-200 nm and α_2-α_2 spacings (λ_α) of 200-500 nm, and are dominated by γ/α_2 interfaces. This characteristic microstructure forms by extruding P/M Ti-47Al-2Cr-2Nb alloys above Tα, and also forms with finer colony size but slightly coarser fully-lamellar structures by hot-extruding similar I/M alloys. Alloying additions of B and W refine λ_L and λ_α in both I/M Ti-47Al (cast and heat-treated above T_α) or in extruded Ti-47Al-2Cr-2Nb alloys. The ultrafine lamellar structure in the P/M alloy remains stable during heat-treatment at 900°C for 2h, but becomes unstable after 4h at 982°C; the ultrafine lamellar structure remains relatively stable after aging for >5000 h at 800°C. Additions of B+W dramatically improve the coarsening resistance of λ_L and λ_α in the I/M Ti-47Al alloys aged for 168 h at 1000°C. In both the P/M and I/M Ti-47Al-2Cr-2Nb alloys, these refined-colony/ultrafine-lamellar structures correlate with high strength and good ductility at room temperature, and very good strength at high temperatures. While refining the colony size improves the room-temperature ductility, alloys with finer λ_L are stronger at both room- and high-temperatures. Additions of B+W produce finer as-processed λ_L and λ_α in I/M TiAl alloys, and stabilize such structures during heat-treatment or aging.

DISCLAIMER

INTRODUCTION

Two-phase alloys based on Ti-(46-48)Al-2Cr-2Nb (at.%) are among the current generation of γ-TiAl alloys developed and being tested for high-temperature structural applications [1-7]. The properties driving applications include low density (4 gm/cm^3), good high temperature strength, stiffness and oxidation-resistance, with other properties being comparable to current alloys [1-9]. The mechanical properties of γ-TiAl alloys are very sensitive to microstructure, which in turn varies considerably with changes in minor alloy composition and in processing parameters. The paradox has been trying to balance and optimize both the room-temperature and high-temperature properties. Generally, fully-lamellar, coarse-grained alloys have good high-temperature strength and creep-resistance at up to 800°C, but lack room-temperature tensile ductility. By contrast, duplex, fine-grained alloys have better tensile ductility but poorer fracture-toughness at room-temperature, and lack high-temperature creep-resistance. In 1995, Kim indicated that refined-grained fully-lamellar structures (300 μm grain size, 500 nm lamellar spacing) in an alloy with a composition of Ti-46.5Al-2Cr-3Nb-0.2W (K5) had a significantly better balance of properties at low and high temperatures [2,10].

In 1995, Liu et al. [11] reported very high levels of room-temperature and high-temperature yield strength (YS), 970 MPa at room-temperature and 850 MPa at 800°C, respectively, in a lamellar P/M Ti-47Al-2Cr-2Nb alloy with a unique refined colony and ultrafine lamellar structure. These alloys also exhibit 1.4% tensile elongation and 22 MPam$^{1/2}$ fracture toughness at room-temperature. Wang et al. [12] showed that these same unique P/M TiAl alloys also had outstanding creep-resistance at 760°C. In 1996, Liu et al. [13] showed that I/M Ti-(46-47)Cr-2Cr-2Nb alloys modified with W and B additions and with somewhat similar fully-lamellar microstructures had a YS of 800 MPa with 3-5% tensile ductility and about 30 MPam$^{1/2}$ fracture toughness at room-temperature. Clearly, this data indicates that microstructural control is the key to alloy design of γ-TiAl alloys with good properties.

The purpose of this work is to present in more detail the quantitative microstructural data for the fine γ and α_2 components of these unique lamellar structures in both P/M and I/M alloys, with an emphasis on the overall average interlamellar and α_2-α_2 spacings (λ_L and λ_α, resepectively). Analytical electron microscopy (AEM) microcompositional data for these individual phase lamellae or particles are included, for clear phase identification and to better determine the nature of the processing-induced microstructure. Effects of variations in processing, heat-treatment and alloy composition on formation of the initial lamellar structures are investigated. In addition, some data on short-term heat-treating at 900-1350°C or longer-term aging at 800-1000°C are also included to determine the stability of such structures. Some preliminary correlations between the microstructural data presented here and the mechanical properties data published previously are discussed to determine properties-controlling factors.

EXPERIMENTAL

The Ti-47Al-2Cr-2Nb (73-1) -325 mesh alloy powder was produced by Pratt &Whitney (West Palm Beach, FL) using their rotary atomization facility with a helium atmosphere. Alloy compositions are listed in Table 1, and processing and heat-treatment conditions are given in Table 2. Wet chemical analysis showed that the powder contained 800 wt. ppm oxygen, 270 wt. ppm carbon and 35 wt. ppm nitrogen. Titanium cans with 15 kg of powder were extruded at T_1 below the α-transus temperature (T_α) and at T_2 above T_α (super-α extrusion), and air cooled. Differential scanning calorimetry data (20°C/min heating, Ar atmosphere) were used to determine the α-transus temperature, which was 1320°C. Pieces of the 20 mm diam. extruded rod were heat-treated or aged in vacuum, and then furnace cooled.

The Ti-47Al alloys with and without B and W additions (designated TIA-16, -17 and -18) were prepared as small (175 g) arc-melted, drop-cast ingots

with an argon cover gas. The ingots were cut and heat-treated at 1400°C for 1h and furnace-cooled. Specimens were then aged for 166 h at 800, 1000 and 1200°C in vacuum. The series of modified Ti-47Al-2Cr-2Nb alloys (TIA-20, -21 and -25) were prepared as larger (260 g, 25 mm diam., 125 mm long) arc-melted, drop-cast ingots, then canned in molybdenum and hot-extruded at T_2 and T_3 above the T_α (Table 2). Specimens were heat-treated at 900-1350°C for 2h in vacuum and then furnace-cooled.

Wafers 0.25 mm thick were cut from the cast ingots, from tested tensile specimen shoulders, or from extruded stock perpedicular to the extrusion direction, and then 3 mm diam. disks were cut by EDM for transmission electron microscopy (TEM) analysis. TEM specimens were electropolished in a twin-jet unit using a solution of 6% perchloric acid, 60% methanol, 33.5% butyl cellusolve, and 0.5% glycerin at -20°C and 32 V. Conventional TEM was performed on a Philips CM30 (300 KV) microscope. Electropolished TEM disks were also examined in a Hitachi S4100/field-emission gun (FEG) scanning electron microscope (SEM).

Lamellar microstructural parameters were measured for most specimens by examining up to three different, representative colonies, and tilting each grain so that the lamellar interfaces were parallel to the electron beam direction (**Z**) with **g** at or near $<111>_\gamma$. Strong diffracting conditions ($s \geq 0$) were used to image all the lamellar interfaces, while weaker diffracting conditions ($s >> 0$) were used to better distinguish the α_2 phase lamellae. Average lamellar spacing (λ_L, including both γ and α_2 lamellae) and α_2-α_2 spacing (λ_α) were measured using a line-intercept method with >100 lamellae in the field of view. Several of the largest and smallest of each lamellar phase constituent in each analyzed area/colony were also measured to establish the maximum representative size range.

Microcompositional analysis of individual phase lamellae within colonies of selected specimens was performed using X-ray energy dispersive spectroscopy (XEDS) on a Philips 400T AEM (FEG, 100KV, probe-size <

10nm). XEDS analysis of coarser intercolony phase consituents was done on a Philips CM12 (LaB_6, 120KV). XEDS peak intensity data were quantified using a standardless method, but *k*-factors for aluminum were checked against a known standard, as recommended by Ramanujan et al. [14,15].

RESULTS

A. Hot-Extruded P/M Ti-47Al-2Cr-2Nb (73-1) Alloys

P/M 73-1 alloy consolidated by hot-extrusion at temperature T_1 well below the T_α has a very fine-grained (<2 μm), duplex structure with some remaining porosity (Fig. 1a). Some details of this microstructure have been presented elsewhere [11], but such material had poor mechanical properties, so further analysis was not done. By contrast, the same material consolidated by super-α extrusion at T_2 above T_α is fully dense, with very close to a fully-lamellar structure (Fig. 1b). The lamellar structure consists of a unique combination of refined colony size (70 μm) with very little intercolony γ (1-3 μm thick, <5 vol.%), and an ultrafine lamellar structure within the colonies. Quantitative lamellar microstructural data are given in Table 3. Optically, this structure would be classed as fully-lamellar, and will be referred to as such for comparison with other work; only electron microscopy reveals the very thin intercolony γ microstructural constituent.

The as-extruded lamellar structure consists of a very uniformly spaced distribution of alternating γ and α_2 phase lamellae (Fig. 2a). The overall λ_L is about 100 nm and λ_α is 220 nm. The γ lamellae are typically 100-200 nm wide, with some being as wide as 500 nm and containing twin subboundaries (Fig. 2b). The α_2 lamellae are always much thinner (20-76 nm). This ultrafine lamellar structure is dominated by γ/α_2 boundaries with few γ/γ twins; this structural feature is shown more clearly in the series of bright-field and dark-field TEM images shown in Fig. 3. These ultrafine γ and α_2 lamellae all have

the same characteristic (111)γ // (0001)α_2 and <110>γ // <1120>α_2 crystallographic habit relationship between close-packed planes and directions in those respective phases that has been shown by others in coarser lamellar structures [9]. Finally, these ultrafine lamellae are relatively straight and free of structural imperfections (kinks, jogs, subboundaries, etc. [15]) across the length of the colonies.

A heat-treatment of 2h at 900°C has little effect on the as-extruded structure and, therefore, was choosen as the "standard" stress-relief treatment. Broader studies of heat-treatments affects at temperatures ranging from 800 to 1325°C for 1-4 h indicated that 900°C was an upper limit for not changing the as-extruded microstructure [11]. By comparison, a heat-treatment of 4 h at 982°C does slightly coarsen the intercolony γ, increasing λ_L to 180 nm and also increasing λ_α. More importantly, the previous thin, continuous α_2 lamellae are now thinner and discontinuous (Fig. 4). Such behavior definitely indicates partial dissolution of the α_2 phase as the overall lamellar structure begins to coarsen.

Heat-treatments just above and below T_α have different effects on the refined colony size and the ultrafine lamellar spacing of the as-extruded material. A heat-treatment of 2 h at 1320°C, just below T_α, does not change the colony size, but considerably coarsens the lamellar structure (Fig. 5a and 5c, and Table 3). Both λ_L and λ_α increase by more than a factor of 4. By contrast, a heat-treatment of 1350°C above T_α coarsens the colony size greatly, but λ_L and λ_α increase by only a small amount.

Specimens of the as-extruded P/M Ti-47Al-2Cr-2Nb alloy (+2 h at 900°C) were aged at 800 and 1000°C for times ranging from 72 to 5040 h. Aging for 5040 h at 1000°C removed the ultrafine lamellar microstructure completely, whereas similar aging at 800°C produced little change (Table 3 and Fig. 6) [16]. No microstructural change could be detected by TEM analysis of specimens

aged for 2160 h at 800°C, whereas subtle changes in λ_L and λ_α were detectable after 5040 h. The increase in λ_α is larger that the change in λ_L, and the appearance of fragmented α_2 laths indicates that α_2 lamallae are dissolving (Fig. 6b). Detailed examination of the lamellar boundary structure reveals the early stages of continuous coarsening of the ultrafine lamellar structure (Fig. 6c) [14,17].

Finally, AEM microcompositional analysis of individual lamellar and intercolony phases was performed in the as-extruded 73-1 alloy after heat-treatments of 2 h at 900°C and of 4 h at 982°C (Table 4). The 73-1 alloy heat-treated at 900°C showed very little coarse α_2 particles within the intercolony γ. The intercolony γ consistently showed close to 50 at% Al, and slightly more Al than Ti, consistent with it being the first phase to form very near T_α. The γ lamellae show a small, but reproducible, phase compositional difference (47 at% Al and closer to 50 % Ti), which would be consistent with those lamellae forming at a larger value of undercooling farther from Tα, as suggested by Kim [2]. The α_2 lamellae have an average of nearly 40 at% Al and more Cr (2 times more) that the γ. The 73-1 alloy heat-treated at 982°C shows no difference in its intercolony γ composition, but does show different compositions for the increased number of coarse intercolony α_2 particles that form. These new α_2 particles clearly have less Al and less Cr than the few α_2 particles which were found in the as-extruded material heat-treated at 900°C. These γ and α_2 phase compositions measured by AEM in the initial microstructure fall within the range of recent phase composition measurements made on a similar alloy by Larson et al. [18,19] using atom probe field-ion microscopy. These data support the suggestion of both Ramanujan et al. [14] and Larson et al. [18] that the initial lamellar structure forms with non-equilibrium phase compositions. More AEM measurements of lamellar phase compositions in other heat-treated and aged specimens of this same 73-1 alloy are in progress.

B. *Cast /M Ti-47Al Alloys (TIA-16, -17, -18) with W and B Additions*

Quantitative lamellar microstructural data on these coarse-grained (100-300 μm) as-cast and heat-treated alloys are given in Table 5. This data has been presented in more detail elsewhere [14,17]. However, a summary is also included here because these data clearly show how B and W microalloying additions (Table 1) affect α_2 lamellar formation, and they also reveal how important the stability of the α_2 lamellae are to the resistance to continuous lamellar coarsening during aging.

Additions of W+B together uniformly refine the lamellar structure that forms when these alloys are heat-treated above T_α at 1400°C (Table 5). The addition of B alone to the Ti-47Al base alloy also significantly refines the lamellar structure (Table 5), but the α_2 lamellae are fragmented and discontinuous (Fig. 7a and 7b), relative to the more uniform and continuous α_2 lamellae found in the W+B modified alloy. It is important to note that these alloys all have the same slow furnace cooling rate; therefore, these results reveal the importance of alloying effects on lamellar refinement, in contrast to the cooling rate effects that have benn shown previously [2].

During thermal aging for 168 h at 1000°C, the Ti-47Al alloy modified with W+B shows much greater resistance to continuous lamellar coarsening than the other alloys (Table 5, Fig. 7c and 7d). The TIA-18 alloy shows no change in λ_L during aging, and only a small increase in λ_α. Detailed TEM analysis indicates that dissolution of the finest α_2 lamellae is the first step in continuous lamellar coarsening; the addition of W makes the fine α_2 lamellae more resistant to dissolution.

Finally, quantitative AEM microcompositional data of individual lamellar phases in the TIA-17 (B) and -18 (W+B) alloys are also given in Table 6 [14]. The compositions for both α_2 and γ lamellae of fresh, as-heat-treated material are consistent with the lamellar compositions found in the P/M Ti-47Al-2Cr-2Nb

alloy, particularly the Al concentrations of each phase. Despite significant differences in the degree of lamellar coarsening in the TIA-17 and -18 alloys, both show the same lower aluminum content in the α_2 phase after aging for 168 h at 1000°C. These data add further support to the claim that the initial ultrafine lamellar structures form with metastable, rather than equilibrium, phase compositions due to the degree of undercooling required to nucleate γ. Maziasz et al. [17] suggest that the non-equilibrium partitioning (rejection) of W by growing γ lamellae produces the W enrichment found in the α_2 lamellae initially. Larson et al. [18] have also independently measured W enrichment to the α_2 lamellae, and have also observed W segregation to α_2/γ interfaces in such fresh lamellar structures of the W-containing TIA-21 alloy (Table 1). The initial W enrichment of the α_2 lamellae is suggested to be one reason why these lamellar structures are more resistant to continuous coarsening [17]. Tungsten diffusion from the α_2 phase may be a necessary step prior to dissolution and coarsening. The lower Al content of the α_2 lamellae in aged TIA-17 and -18 alloys is also consistent with similar compositional changes found in the α_2 lamellae of P/M Ti-47Al-2Cr-2Nb heat-treated at 982°C (Table 4).

B. *Hot-Extruded I/M Ti-(46-47)Al-2Cr-2Nb Alloys (TIA-20, -21, -25) with W and B Additions*

Quantitative lamellar microstructural data on these fine-grained I/M alloys hot-extruded at T_2 or T_3 ($T_3<T_2$) above T_α, and heat-treated at either 900°C or 1320°C are given in Table 7, and can also be found elsewhere [20,21]. These particular data demonstrate the synergy between alloy (B+W additions) and processing conditions (temperature above T_α) in their effect on the formation of the ultrafine lamellar microstructure, particularly λ_α.

Hot-extrusion of these I/M TiAl alloys at T_2 and T_3 produces relatively fine colony sizes of 25-35 μm [20], and relatively fine lamellar structures (λ_L<200 nm,

Table 7). Heat-treatment for 2 h at 1320°C does not significantly coarsen the grain size, but does appreciable coarsen the lamellar structure (λ_L- 300-400 nm, Table 7), similar to the behavior observed in the P/M Ti-47Al-2Cr-2Nb alloy. The lamellar structure of TIA-20 (B) extruded at T_3 was a non-uniform mixture of coarser and finer lamellar patches within any given colony, including some very coarse γ lamellea. The TIA-21 (W+B) alloy forms a more uniform fine lamellar structure, with slightly smaller values of λ_L and λ_α , when extruded at the higher temperature (T_2). The lamellar structures in these I/M TIA- series alloys, however, are still not as fine and contain more γ/γ twins (and hence lower relative γ/α_2 boundary fraction) relative to the P/M Ti-47Al-2Cr-2Nb alloy extruded at T_2 (compare Figs. 2b and 8a). The TIA-25 alloy, with W+B and 46 instead of 47 at.% Al, has both a finer λ_L (105 nm) and λ_α (215 nm) compared to the TIA-21 alloy after extrusion at T_2 (Fig. 8b and Table 7). The TIA-25 alloy still has some lamellar nonuniformity (some clusters of very fine α_2 lamellae), but has a more evenly spaced structure with far fewer γ/γ twins compared to alloy TIA-21. The I/M TIA-25 alloy (W+B) comes closest to achieving the ultrafine lamellar structure quality found in the P/M Ti-47Al-2Cr-2Nb alloy, but with a significantly smaller colony size (26 μm).

DISCUSSION

A. Correlations Between Microstructures and Mechanical Properties

While these unique refined-colony/ultrafine lamellar microstructures are new and interesting, they are also important because they produce an outstanding balance of mechanical properties in these two-phase γ-TiAl alloys at room and elevated temperatures [11,13,20]. The P/M Ti-47Al-2Cr-2Nb alloy (extruded at T_2 and heat-treated at 900°C) has 1.4% total tensile elongation (Fig. 9), YS of 970 MPa, and fracture toughness of 22 $MPam^{1/2}$, all at room-temperature [11]. Heat-treatment of the P/M alloy at 1320°C increases the

elongation to 3.6%, but lowers the YS to 650 MPa [16]. The I/M TIA-20 and -21 alloys (extruded at T_3) have total elongations 4.6 and 3.0%, and YS of 666 and 790 MPa, respectively [13]. Extrusion of TIA-21 at T_2 raises its ductility slightly to 4% (Fig. 9), whereas heat-treatment at 1320°C produces little change in ductility (Fig. 9) and significantly decreases YS [13]. The I/M TIA-25 alloy (extruded at T_2) also shows 4% ductility (Fig. 9), but with a higher YS of 890 MPa compared to TIA-21 [20]. Liu et al. [16,20] have explained the improved ductility in these fully-lamellar (FL) γ-TiAl alloys mainly on the basis of refined colony size, with the best ductilities (4-5%) found in alloys with colony sizes <50 μm [20]. Kim [2] noted a similar relationship between colony size and ductility for the FL I/M K5 (Ti-46.5Al-2Cr-3Nb-0.2W) alloy, with colony sizes in the 100-300 μm range producing from 4 to 2 % elongation. Further, Kim [2] identified optimum FL microstructures to include colony/grain sizes down to 50 μm, but indicated that such grain sizes are difficult to achieve.

One remarkable feature of the room-temperature mechanical properties data on these P/M and I/M refined-colony/fully-lamellar alloys is the fact that they have *both* high strength and relatively high tensile ductility [2,11]. Kim [2] notes the much higher Hall-Petch slope for YS as a function of grain size for FL as compared to duplex TiAl alloys, indicating significantly different fundamental strength-controlling mechanisms in the two different kinds of processing-induced microstructures. Indeed, the data for our refined-colony P/M Ti-47Al-2Cr-2Nb fall about on the same Hall-Petch line, but at twice the level of strength observed previously. Liu et al. [11] explained the very high strength of this P/M material as similar to a micro-laminate, strengthened by the ultrafine and fairly regularly alternating γ and α_2 platelets (Fig. 2b). More recently, Liu and Maziasz [16,20] noted that these ultrafine I/M and P/M alloys have a Hall-Petch relationship between YS (room-temperature) and λ_L , as shown in Fig. 10, plotting the microstructural data from Tables 3 and 7. Clearly, the alloys with the finest λ_L are the strongest, indicating that λ_L controls the strength of these two-

phase alloys. As has been noted previously [11], the λ_L values for the ultrafine lamellar structures observed in this work are significantly smaller than have been observed previously in cast TiAl alloys, and are finer that the λ_L values of 200-500 nm observed by Kim [2,22] and Fuchs [23,24] in alloys (K5 or Ti-47Al-1Cr-1V-2.5Nb, and P/M Ti-48Al-2Cr-2Nb, respectively) processed near or above T_α. Fuchs [23] in particular found 2.9% elongation, but a YS of only 412 MPa for P/M Ti-48Al-2Cr-2Nb with λ_L of 650 nm (22 μm colony size).

Even more important tha the strength found in these ultrafine lamellar TiAl alloys at room- temperature, is the strength that they retain at high temperatures of 800-1000°C. The P/M Ti-47Al-2Cr-2Nb alloys have a YS of over 800 MPa at 800°C [11]. The I/M TIA-20(T_3), -21(T_2) and -25(T_2) alloys have YS of 560, 730 and 750 MPa, respectively [13,20]. Typical YS values found in other fully-lamellar two-phase γ-TiAl alloys at 800°C are about 300-400 MPa, with W-modified alloys like the K5 alloy being among the strongest of those [2,10,22-24]. Clearly, the ultrafine lamellar alloys are much stronger at higher temperatures than similar fully-lamellar alloys with λ_L >500 nm. Within this relatively narrower group of ultrafine lamellar I/M and P/M alloys based on the Ti-47Al-2Cr-2Nb composition, YS at 800°C also scales directly with λ_L on a Hall-Petch plot (Fig. 11). Within this limited data set, alloys with the highest YS also have the finest λ_α values, in the range of 200-400 nm. This suggests that both λ_α , as well as λ_L , may be even more important for determining high-temperature strength than it is for strengthening at room-temperature.

Creep-resistance is a very important measure of in-service lifetime for many TiAl applications. Creep data at 760°C on the ultrafine lamellar P/M Ti-47Al-2Cr-2Nb alloy by Wang, et al. [12] show that this material also has outstanding creep resistance (Fig. 12). The creep data for other γ-TiAl alloys with 47-48 at.% Al includes data which show that fully-lamellar material has much better creep-resistance than duplex material. These same creep data

also show that W-modified TiAl alloys have better creep resistance than alloys without W [2,25-27]. The ultrafine lamellar P/M TiAl alloy far exceeds the creep-strength of the other alloys despite their finer colony size, so that the creep-strength is directly attributable to their fine λ_L within the colonies. Wang et al. [12] explain their high creep strength by suggesting that the small λ_L (shown in Fig. 2b) causes the γ lamellae to be too narrow for Orowan bowing of matrix dislocations, and causes pinning of those dislocation segments at the α_2/γ interfaces at low creep stresses. Hsiung and Nieh [28] have further analyzed those creep-induced dislocation structures, and suggest that both the interfacial pinning, as well as the obstacles created by secondary slip of dislocations within the γ lamellae, produce the observed creep strength. Soe et al. [29] in a different study of primary creep in investment-cast Ti-47Al-2Nb-2Mn with 0.8 % TiB_2 and much coarser lamellar structures also find that finer λ_L correlates with improved creep-resistance at 760°C.

B. *Formation and Stability of the Ultrafine Lamellar Structures*

Because these unique, new microstructures produce such a remarkable combination of mechanical properties, the effects of both alloying and processing on their formation and stability are also very important.

In terms of formation, all of the TiAl alloys characterized here appear to fall into category of Type I near-lamellar microstructures described by Kim [30]. Such microstructures form by heating or processing the TiAl alloy above T_α, and then the γ lamellae nucleate in the α-grains as the alloy is undercooled. Generally, increasing the cooling rate (larger undercooling) decreases λ_L until the massive transformation of α to γ occurs to prevent formation of the fully-lamellar structure [30-32]. The residual disordered α phase trapped between the γ lamellae then transforms to α_2 below the eutectoid temperature to produce the final lamellar microstructure. For binary TiAl alloys, such fully-lamellar

structures form more readily in Ti-47Al alloys than in alloys with less Al, and are also more resistant to discontinuous coarsening during aging [33]. Generally, slow furnace cooling rates produce λ_L of 1 μm or more in binary TiAl alloys, and polysynthetically twinned TiAl crystals have lamellar structures with λ_L slightly less than 1-2 μm and λ_α of 5-10 μm, dominated by γ/γ interfaces [8, 31-34]. Kim [30] has reported an ultrafine lamellar structure with λ_L of 0.03-0.2 μm in a Ti-47Al-1Cr-1V-2.5Mo alloy heat-treated above T_α. Soe et al. [29] also report λ_L of 0.3 μm and λ_α of about 1 μm in investment-cast Ti-47Al-2Nb-2Mn with 0.8 % TiB_2. Generally, there are no systematic studies of comparable alloys with near- or fully-lamellar structures as consistently fine as reported here.

The ultrafine lamellar microstructure forms easily in the P/M Ti-47Al-2Cr-2Nb alloy processed above T_α. Additions of W+B refine both λ_L and λ_α in the I/M Ti-47 alloys heat-treated above T_α, and make the α_2 lamellae more continuous. This particular effect has been interpreted as B additions increasing the γ lamellae nucleation rate without much affect on growth of those lamellae, according to the Type I lamellar formation mode [21]. By contrast, the addition of W+B appears to retard the growth of the γ lamellae in addition to increasing their nucleation rate, resulting in a refined λ_L that also includes more continuous α_2 lamellae. Rejection of W by the γ lamellae could retard their growth, and would also be consistent with the γ/α_2 interfacial W segregation observed by Larson et al. [18], as well as the W partitioning to the α_2 lamellae observed by AEM (Table 6). In the more complex I/M Ti-47Al-2Cr-1.8Nb-0.2W-0.15B (TIA-21) alloy, increasing the processing temperature above T_α refines the lamellar structure and makes it more uniform, consistent with formation behavior discussed above. The TIA-25 alloy was produced with slightly less Al in order to increase the amount of α_2 within the ultrafine structure. Both λ_L and λ_α were successfully refined further, and they both remained continuous in this

alloy. This demonstrates that alloying affects can help control λ_α in order to obtain such ultrafine lamellar structures at slower cooling rates.

The ultrafine lamellar structures that form during cooling of the as-processed material must also remain stable during subsequent heat-treatment and thermal aging to provide technologically relevent improvements in high-temperature strength. In fact it is somewhat of a paradox for finer lamellar structures to be more stable, because reducing the surface area of the structure is one of the driving forces for continuous lamellar coarsening [33]. However, two details of these ultrafine lamellar structures that appear to be most important to their stability and coarsening resistance at high-temperatures are the resistance of the original fine α_2 lamellae to dissolution and the metastable composition of those α_2 lamellae, both of which are interrelated. For the P/M Ti-47Al-2Cr-2Nb alloys, heat-treatment at near 1000°C begins to change the original ultrafine lamellar structure after only 4 h, with both dissolution of the α_2 and compositional changes consistent with the equilibrium phase composition at that temperature (less Al) occurring simultaneously. Thermal aging of that material at 1000°C for >5000 h completely removes the ultrafine lamellar structure, whereas similar aging at 800°C produces only subtle changes. Such behavior is consistent with the kinetics of diffusion being much more sluggish at the lower aging temperature, and with the α_2 lamellae needing to get closer to their equilibrium phase composition before they can dissolve.

This same argument can also consistently be extended to explain the improved aging resistance of the W+B modified simpler Ti-47Al alloys. Tungsten is also forced into the metastable α_2 lamellae when they form, and apparently is repartitioning much more slowly during aging at 1000°C than the Al [14,17] (Table 6). The ratio of $[conc.W]_\gamma/[conc.W]_\alpha$ is 0.66 in fresh material, 1.0 in material aged 168 h at 1000°C, and 2.3 in spheroidized, completely non-lamellar material aged 168 h at 1200°C. The later specimen suggests that at equilibrium, the α_2 should have less W than the γ matrix rather than more, in

support of the non-equilibrium nature of the initial ultrafine lamellar structure. This suggests that W segregation to the fine α_2 lamellae is part of what makes them fine in the first place, and then also makes them more resistant to dissolution during aging. The longer the α_2 lamellae resists dissolution during aging, the longer the ultrafine lamellar structure resists continuous coarsening. While λ_L may be the strength-controlling factor at any point in time, the role of the α_2 lamellae seems to hold these ultrafine lamellae together and make them stable at elevated temperatures. Aging experiments on the newer and more complex I/M TIA-21 and -25 alloys modified with both B and W are in progress. Additional experiements to determine the stability of such microstructures during creep are also needed.

To summarize, achieving refined-colony/ultrafine-lamellar microstructures has enabled a combination of ductility and strength at room-temperature, and strength and creep-resistance at high-temperatures that has not been achieved previously in lamellar two-phase γ-TiAl alloys. The refined colony size makes these alloys ductile, while the ultrafine λ_L makes them strong. These data on processing above T_α and effects of alloying additions of W and B demonstrate that controlling and stabilizing the lamallar structure in general, and the fine α_2 component in particular, is an important part of any alloy design strategy aimed at improving the properties of γ-TiAl alloys.

CONCLUSIONS

1. Hot-extrusion of P/M and I/M Ti-47Al-2Cr-2Nb alloys at T_2 above T_α produces near fully lamellar structures with a refined colony size and ultrafine λ_L and λ_α.
2. Such microstructures do not change after heat-treatment of 2h at 900°C, whereas λ_L and λ_α coarsen considerably at 1320°C with no change in colony

size. Such structures in P/M Ti-47Al-2Cr-2Nb are quite resistant to lamellar coarsening during aging at 800°C for >5000 h.

3. For I/M Ti-47Al-2Cr-2Nb alloys extruded at T_2, additions of W+B refine λ_L significantly, with only a slight refinement of λ_α. The same additions of W+B to a similar alloy with 46 at.% Al produce a significant refinement in both λ_L and λ_α.

ACKNOWLEDGEMENTS

Thanks to D.S. Easton, L. Heatherly, K.S. Blakely, and C.A. Carmichael for alloy preparation and fabrication, and J.L. Wright for heat treating, mechanical properties and metallography. Thanks to J.W. Jones for preparing specimens for electron microscopy. Thanks to D. Clemens at Pratt &Whitney, Advanced Engineering Operations, West Palm Beach, FL, for producing TiAl powders and support of the CRADA work. Thanks to P. Angelini for program management support for both the DP-CRADA and the Advanced Industrial Materials (AIM) work. Thanks to D.J. Alexander and D.J. Larson for reviewing the manuscript. Research sponsored by the U.S. Department of Energy, Assistant Secretary for Energy Efficiency and Renewable Energy, Office of Industrial Technologies, AIM Program, and Assistant Secretary of Defense Programs (DP), Technology Management Group, Technology Transfer Initiative, under contract DE-AC05-96OR22464 with Lockheed-Martin Energy Research Corp.

REFERENCES

1. Y-W. Kim, *JOM*, 1994, vol. 46, pp. 30-40.
2. Y-W. Kim: in *Gamma Titanium Aluminides*, eds. Y-W. Kim, R. Wagner, M. Yamaguchi, TMS, Warrendale, PA, 1995, p. 637-654.
3. Y-W. Kim: in *High-Temperature Ordered Intermetallics Alloys IV*, eds. L.A. Johnson, D.P. Pope and J.O. Stiegler, MRS, Pittsburgh, PA, 1991, vol. 213, pp. 777-794.
4. D.M. Dimiduk: in *Gamma Titanium Aluminides*, eds. Y-W. Kim, R. Wagner, M. Yamaguchi, TMS, Warrendale, PA, 1995, p. 3-20.
5. C.M. Austin and T.J. Kelly: in *Gamma Titanium Aluminides*, eds. Y-W. Kim, R. Wagner, M. Yamaguchi, TMS, Warrendale, PA, 1995, p. 21-40.
6. R. Wagner, et al.: in *Gamma Titanium Aluminides*, eds. Y-W. Kim, R. Wagner, M. Yamaguchi, TMS, Warrendale, PA, 1995, p. 387-404.
7. S. Huang: in *Structural Intermetallics*, eds. R. Darolia, J. Lewandowski, C.T. Liu, P. Martin, D. Miracle and M. Nathal, TMS, Warrendale, PA, 1993, pp. 299-307.
8. M. Yamaguchi and H. Inui: in *Structural Intermetallics*, eds. R. Darolia, J. Lewandowski, C.T. Liu, P. Martin, D. Miracle and M. Nathal, TMS, Warrendale, PA, 1993, pp. 127-142.
9. M. Yamaguchi and Y. Umakoshi, Prog. Mater. Sci. Eng., 1990, 34 (1), pp. 1-148.
10. J. Kumpfert, Y-W. Kim and D.M. Dimiduk, Mater. Sci. and Eng., 1995, A192/193, pp. 465-473.
11. C.T. Liu, et al.: in *Gamma Titanium Aluminides*, eds. Y-W. Kim, R. Wagner, M. Yamaguchi, TMS, Warrendale, PA, 1995, p. 679-688.
12. J.N. Wang, A.J. Schwartz, T.G. Nieh, C.T. Liu, V.K. Sikka, and D.J. Clemens: in *Gamma Titanium Aluminides*, eds. Y-W. Kim, R. Wagner, M. Yamaguchi, TMS, Warrendale, PA, 1995, p. 949-957.
13. C.T. Liu, J.H. Schneibel, P.J. Maziasz, J.L. Wright and D.S. Easton, *Intermetallics*, 1996, 4, pp. 429-440.
14. R.V. Ramanujan, P.J. Maziasz and C.T. Liu, *Acta Mater.*, 1996, 44 (7), pp. 2611-2642.
15. R.V. Ramanujan and P.J. Maziasz, *Met. and Mater. Trans. A*, 1996, 27A, pp. 1661-1673.
16. C.T. Liu and P.J. Maziasz, unpublished data, ORNL, 1995, presented at Symposium on Intermetallic Compounds at the JIM '95 Meeting, December 13-15, 1995 in Honolulu, HA.
17. P.J. Maziasz, R.V. Ramanujan, C.T. Liu and J.L. Wright, *Intermetallics*, 1997, 5, pp. 83-95.
18. D.J. Larson, C.T. Liu and M.K. Miller, "Tungsten Segregation in $\alpha_2+\gamma$ Titanium Aluminides," *Intermetallics* , to be published in 1997.
19. D.J. Larson, C.T. Liu and M.K. Miller, "Boron Solubility and Boride Compositions in $\alpha_2+\gamma$ Titanium Aluminides," *Intermetallics* , to be published in 1997.

20. C.T. Liu, P.J. Maziasz and J.L. Wright, "Key Microstructures Controlling the Mechanical Properties of Two-Phase TiAl Alloys With Lamellar Structures," to be published in Proc. Symp. *High-Temperature Ordered Intermetallic Alloys VII*, MRS, Pittsburgh, PA in 1997.
21. P.J. Maziasz and C.T. Liu, "Ultrafine Fully-Lamellar Structures in Two-Phase γ-TiAl Alloys," to be published in Proc. Symp. *High-Temperature Ordered Intermetallic Alloys VII*, MRS, Pittsburgh, PA in 1997.
22. Y-W. Kim: *Matls. Sci. and Engin.* , 1995, A192/193, pp. 519-533.
23. G.E. Fuchs, in *High-Temperature Ordered Intermetallic Alloys VI*, eds. J.A. Horton, I. Baker, S. Hanada, R.D. Noebe, and D.S. Schwartz, MRS, Pittsburgh, PA, 1995, vol. 364 (part 2), pp.799-804.
24. G.E. Fuchs: in *Gamma Titanium Aluminides*, eds. Y-W. Kim, R. Wagner, M. Yamaguchi, TMS, Warrendale, PA, 1995, p. 563-570.
25. G.B. Viswanathan and V.K. Vasudevan: in *Gamma Titanium Aluminides*, eds. Y-W. Kim, R. Wagner, M. Yamaguchi, TMS, Warrendale, PA, 1995, pp. 967-974.
26. J. Beddoes, L. Zhao, J. Triantafillou, P. Au, and W. Wallace: in *Gamma Titanium Aluminides*, eds. Y-W. Kim, R. Wagner, M. Yamaguchi, TMS, Warrendale, PA, 1995, p. 959-966.
27. S.W. Schwenker and Y-W. Kim: in *Gamma Titanium Aluminides*, eds. Y-W. Kim, R. Wagner, M. Yamaguchi, TMS, Warrendale, PA, 1995, p. 985-992.
28. L.M. Hsiung and T.G. Nieh, "Deformation Substructure in a Creep Deformed Lamellar TiAl Alloy," to be published *in Scripta Met. et Mat.* in 1997.
29. D.Y. Seo, T.R. Bieler and D.E. Larson, "Effect of Interstitial Concentration and Heat Treatment on Microstructure and Primary Creep of Investment Cast Ti-47Al-2Nb-2Mn with 0.8 v.% TiB_2," to be published in Proc. Symp. *High-Temperature Ordered Intermetallic Alloys VII*, MRS, Pittsburgh, PA in 1997.
30. Y-W. Kim, *Acta Metall. et Mater.* 1992, 40, pp. 1121-1134.
31. M. Takeyama, T. Kumagai, N. Nakamura, M. Kikuchi; in *Structural Intermetallics*, eds. R. Darolia, J. Lewandowski, C.T. Liu, P. Martin, D. Miracle and M. Nathal, TMS, Warrendale, PA, 1993, pp. 167-176.
32. P. Wang and V.J. Vasudevan; in *High Temperature Ordered Intermetallics V*, ed. I. Baker, R. Darolia, J.D. Wittenberger, and M.H. Yoo, MRS, Pittsburgh, PA, 1993, vol. 288, pp. 229-236.
33. J.D. Livingston and J.W. Cahn, *Acta Met.* , 1974, 22, pp. 495-503.
34. Y. Umakoshi, T. Nakano, and T. Yamane, *Matls. Sci. and Engin.*, 1992, A152, 81-88.

FIGURE CAPTIONS

Fig. 1 - SEM micrographs of P/M Ti-47Al-2Cr-2Nb (73-1) hot-extruded at a) T_1 to produce a duplex structure (metallographically polished and etched surface), and b) at T_2 to produce a refined-grained, fully-lamellar structure (electropolished surface).

Fig. 2 - TEM analysis of P/M Ti-47Al-2Cr-2Nb (73-1) hot-extruded at T_2, showing a) the typical very straight and evenly spaced ultrafine lamellar structure found within each colony (lower magnification), and b) the finer α_2 lamellae found uniformly distributed between most larger γ lamellae (higher magnification).

Fig. 3 - TEM analysis of P/M Ti-47Al-2Cr-2Nb (73-1) hot-extruded at T_2, to show the regular distribution of α_2 in between γ lamellae so that α_2/γ interfaces dominate the structure. a) diffraction patterns from the coincident $<1120>\alpha_2$ and $<110>\gamma$ zone axes with b) schematic to identify various reflections, c) bright-field (BF) image of all lamellae, d) dark-field (DF) image of γ lamellae using matrix reflection (A), e) DF image of γ lamellae using twin reflection (B), and f) DF image of α_2 lamellae using α_2 reflection (C).

Fig. 4 - The effect of heat-treatment at 982°C for 4 h on the lamellar structure of P/M Ti-47Al-2Cr-2Nb (73-1) hot-extruded at T_2, as seen by TEM analysis with lamellar boundaries tilted to show fragmented α_2 lamellae.

Fig. 5 - The effects of heat-treatments on lamellar coarsening and colony size of P/M Ti-47Al-2Cr-2Nb (73-1) hot-extruded at T_2, as seen by SEM analysis of electropolished TEM disks (a, b), and TEM analysis (c,d), for 2h at 1320°C (a,c) and for 2h at 1350°C (b,d).

Fig. 6 - The effect of thermal aging at 800°C for 5040 h on the lamellar structure of P/M Ti-47Al-2Cr-2Nb (73-1) hot-extruded at T_2. TEM analysis with a) strong contrast (**9**=$<111>\gamma$) showing all lamellar boundaries parallel to electron beam direction (**z**), b) contrast showing only α_2 lamellae, tilted 10-15° to show fragmented appearance, and c) higher magnification near **g**=$<111>\gamma$ showing dislocation and lamellar boundaries that reveal α_2 dissolution and continuous lamellar coarsening.

Fig. 7 - The effects of thermal aging at 1000°C for 168 h on the lamellar structures of I/M Ti-47Al alloys modified with B and B+W. TEM analysis of a) TIA-17 (B) and b) TIA-18 (B+W), as-heat-treated at 1400°C for 1 h, and of c) TIA-17 (B) and d) TIA-18 (B+W), aged at 1000°C. Alloy TIA-17 (B) shows evidence of continuous lamellar coarsening, whereas TIA-18 (B+W) is much more resistant to such coarsening.

Fig. 8 - TEM analysis of lamellar structures in I/M TiAl alloys hot-extruded at T_2 and heat-treated at 900°C for 2 h. a) TIA-21 (Ti-47Al-2Cr-1.8Nb-0.2W+B) alloy and b) TIA-25 (Ti-46Al-2Cr-1.8Nb-0.2W+B) alloy, with b) having a somewhat finer distribution of α_2 lamellae than a).

Fig. 9 - Plot of room-temperature tensile ductility (in air) for P/M and I/M TiAl alloys extruded above T_α and heat-treated to either preserve (900°C) or coarsen (1320°C) the ultrafine lamellar structure without changing the refined colony size (30-70 μm) [11,13,16,17].

Fig. 10 - Hall-Petch plot of room-temperature yield-strength versus average lamellar spacing (Tables 3 and 7) for P/M and I/M TiAl alloys extruded above T_α and heat-treated to either retain or coarsen the ultrafine lamellar structure [11,13,16,17].

Fig. 11 - Hall-Petch plot of yield-strength at 800°C versus average lamellar spacing (Tables 3 and 7) for P/M and I/M TiAl alloys extruded above T_α and heat-treated at 900°C for 2 h to retain the ultrafine lamellar structure [11,13,16,17].

Fig. 12 - Creep-resistance, as measured by steady-state creep rate, plotted as a function of creep stress at 760°C for P/M Ti-47Al-2Cr-2Nb hot-extruded at T_2, to produce the refined-colony/ultrafine-lamellar structure, with comparison to creep data of others on a variety of related TiAl alloys, from Wang et al. [12].

TABLE 1 - Alloy Composition (at. %)

Alloy (processing)	Ti	Al	Cr	Nb	W	B
73-1 (P/M)	49	47	2	2		
TIA-16 (I/M)	53	47				
TIA-17 (I/M)	53	47				0.014
TIA-18 (I/M)	52.5	47			0.5	0.014
TIA-20 (I/M)	48.85	47	2	2		0.15
TIA-21 (I/M)	48.85	47	2	1.8	0.2	0.15
TIA-25 (I/M)	49.85	46	2	1.8	0.2	0.15

TABLE 2 - Alloy Processing and Heat-Treatment Conditions

Alloy(s)	Processing	Heat-Treatment
73-1 (P/M)	hot-extrusion $T_1<T\alpha$	
	hot-extrusion $T_2>T\alpha$	2h at 900°C 4h at 982°C 2h at 1320°C 2h at 1350°C
TIA-16, 17, 18 (I/M)	as-cast	1h at 1400°C
TIA-20 (I/M)	hot-extrusion $T_3>T\alpha$	2h at 900°C 2h at 1320°C
TIA-21 (I/M)	hot-extrusion $T_3>T\alpha$	2h at 900°C 2h at 1320°C
	hot-extrusion $T_2>T\alpha$	2h at 900°C
TIA-25 (I/M)	hot-extrusion $T_2>T\alpha$	2h at 900°C

$T_3<T_2$

Table 3 - Quantitative Lamellar Microstructural Data on Hot-Extruded and Heat-Treated P/M Ti-47Al-2Cr-2Nb Alloys

Extrusion/Heat-Treatment	Interlamellar spacing (nm)	α_2-α_2 spacing (nm)	γ-width (nm)	α_2-width (nm)
T_2/ none	100	220	100-500	20-76
T_2/ 2 h at 900°C	similar to above			
T_2/ 4 h at 982°C	180	325	60-600	20-60
T_2/ 2 h at 1320°C	390 (±75)	900 (±300)	80-2000	70-400
T_2/ 2 h at 1350°C	140	300	50-300	70-430
T_2/ 2 h at 900°C + aged >5000 h at 800°C	120	285	70-630	15-45

Table 4 - Quantitative Microcompositional Analysis of Phases in P/M Ti-47Al-2Cr-2Nb Alloys

Extrusion/Heat-Treatment	Phase	Composition (at.%) Al	Ti	Cr	Nb
T_2/ 2 h at 900°C	lamellar γ (8)[a]	47.4	49.2	1.6	1.8
	lamellar α_2 (4)	39	56.3	3	1.7
	equiaxed γ (1)	46.4	50	1.6	2.0
	intercolony γ (9)	49	47.3	1.4	2.3
	intercolony α_2 (1)	40.5	55	2.3	2.2
T_2/ 4 h at 982°C	intercolony γ (3)	47.7	48.4	1.5	2.4
	intercolony α_2 (4)	35[b]	61	1.7	2.3

a - number of individual measurements included in average
b - ± 3.6, which is a typical variation for individual measurements

Table 5 - Quantitative Lamellar Microstructural Data on Heat-Treated and Aged I/M Ti-47Al Alloys

Alloy/Condition	Interlamellar spacing (nm)	α_2-α_2 spacing (nm)	γ-width (nm)	α_2-width (nm)
TIA-16/ 1 h at 1400°C	400	520	200-650	60-120
TIA-17(B)/ 1 h at 1400°C	170	330-500	70-400	50-100
TIA-18(B+W)/1 h at 1400°C	190	420-560	140-720	50-130
TIA-16/ HT + aged 168 h at 1000°C	800-1950	>1300	520-2200	220-1030
TIA-17/ HT + aged 168 h at 1000°C	350-400	1420	200-1200	50-155
TIA-18/ HT + aged 168 h at 1000°C	190	660	150-440	60-130

Table 6 - Quantitative Microcompositional Analysis of Phases in Heat-Treated and Aged I/M Ti-47Al Alloys

Extrusion/Heat-Treatment	Phase	Composition (at.%) Al	Ti	W
TIA-17(B)/ 1 h at 1400°C	lamellar γ (7)[a]	48	52	
	lamellar α_2 (1)	40	60	
TIA-17/ HT + aged 168 h at 1000°C	lamellar γ (3)	48	52	
	lamellar α_2 (4)	36($\pm$0.4)[b]	64	
TIA-18(B+W)/ 1 h at 1400°C	lamellar γ (3)	48	51.4	0.6
	lamellar α_2 (4)	39.4	59.7	0.9
TIA-18/ HT + aged 168 h at 1000°C	lamellar γ (4)	48.7	50.6	0.7
	lamellar α_2 (3)	35.6	63.7	0.7

a - number of individual spot measurements included for determining average value
b - typical $\pm$ σ variation for average of individual measurements

Table 7 - Quantitative Lamellar Microstructural Data on Hot-Extruded and Heat-Treated I/M Ti-47Al-2Cr-2Nb Modified Alloys

Alloy/Condition	Interlamellar spacing (nm)	α_2-α_2 spacing (nm)	γ-width (nm)	α_2-width (nm)
TIA-20(B)/ T_3 + 2 h at 900°C	140-325	400-500	95-870	30-60
/ T_3 + 2 h at 1320°C	440	1000	160-1250	55-265
TIA-21(B+W)/ T_3 + 2 h at 900°C	160	460-500	75-635	20-55
/ T_3 + 2 h at 1320°C	300	800	290-1100	55-210
/ T_2 + 2 h at 900°C	140	400	40-750	15-110
TIA-25(B+W)/ T_2 + 2 h at 900°C	105	215	20-520	15-40

$T_3<T_2$

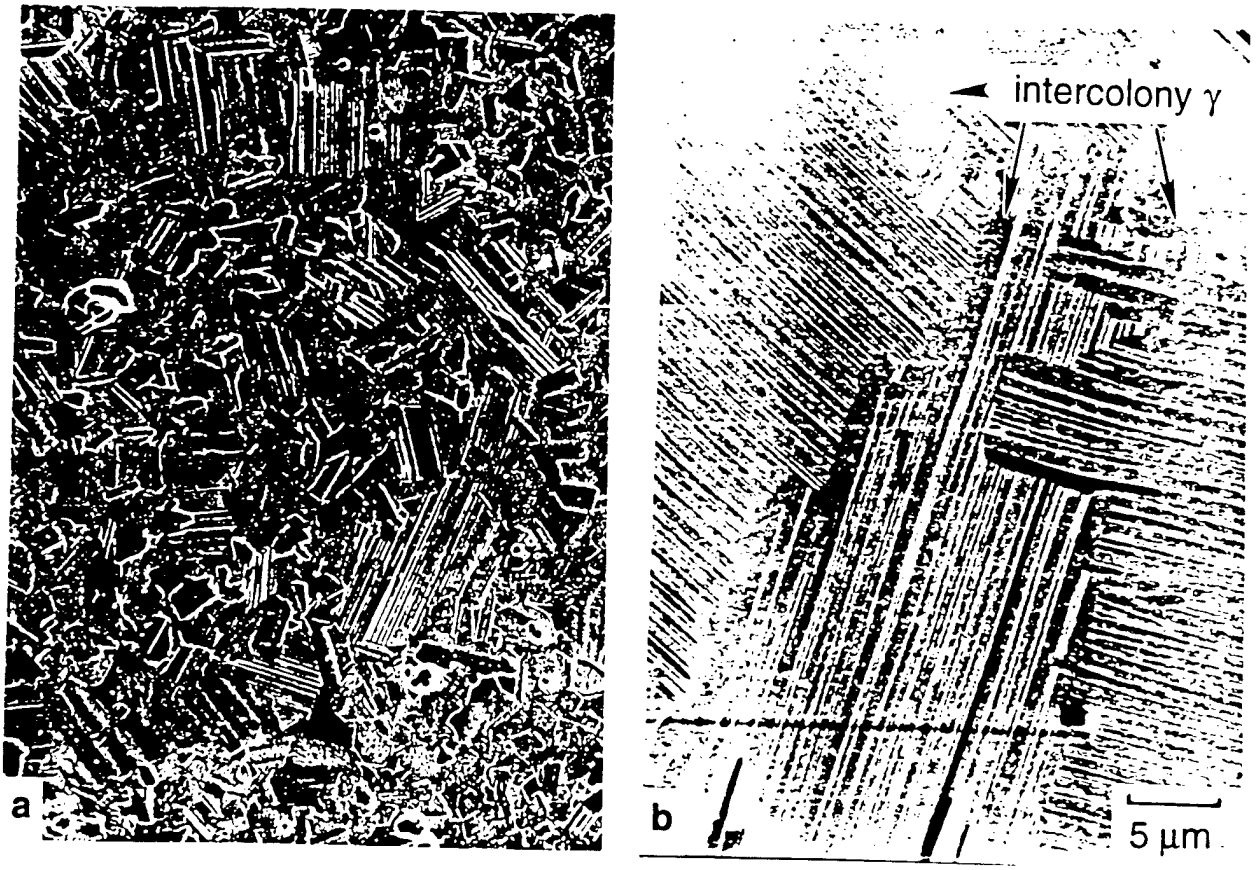

Fig. 1

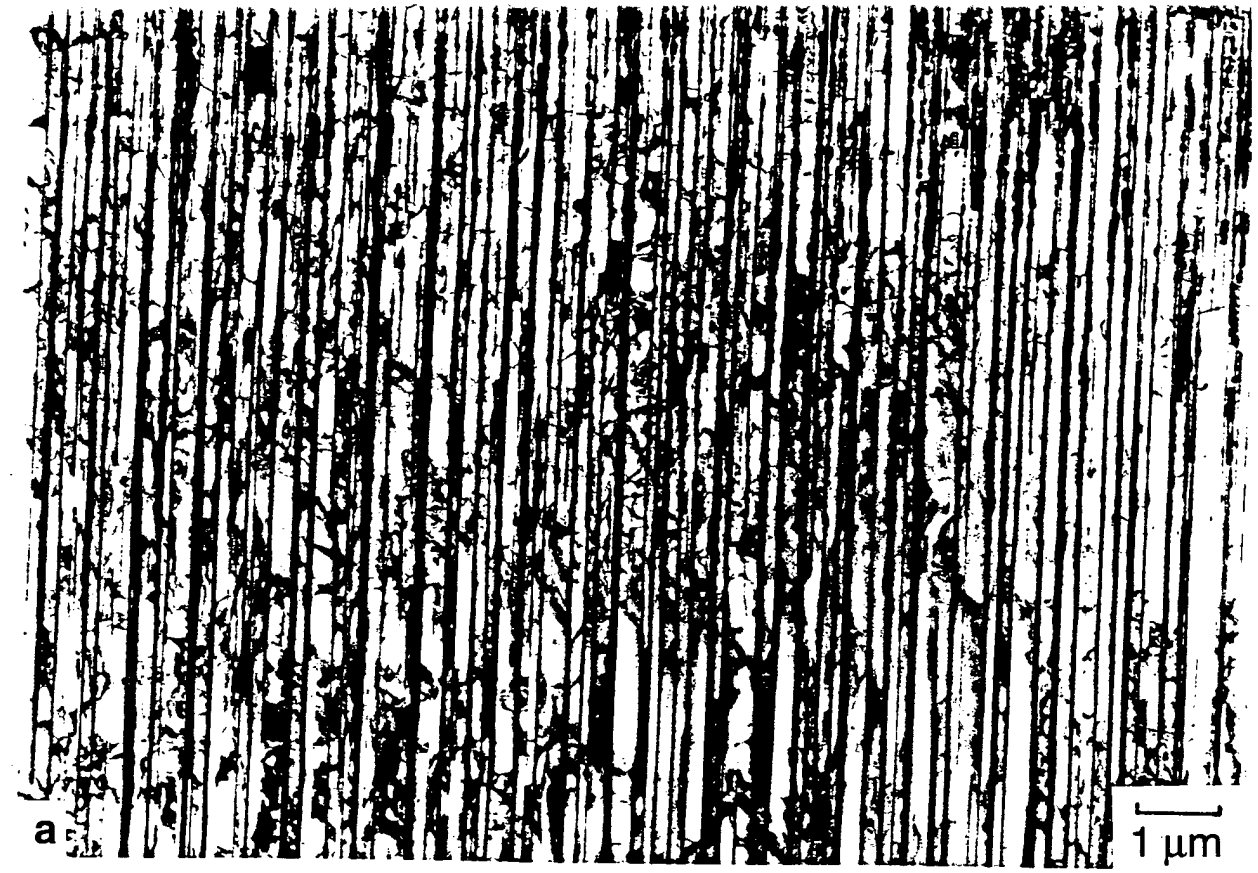

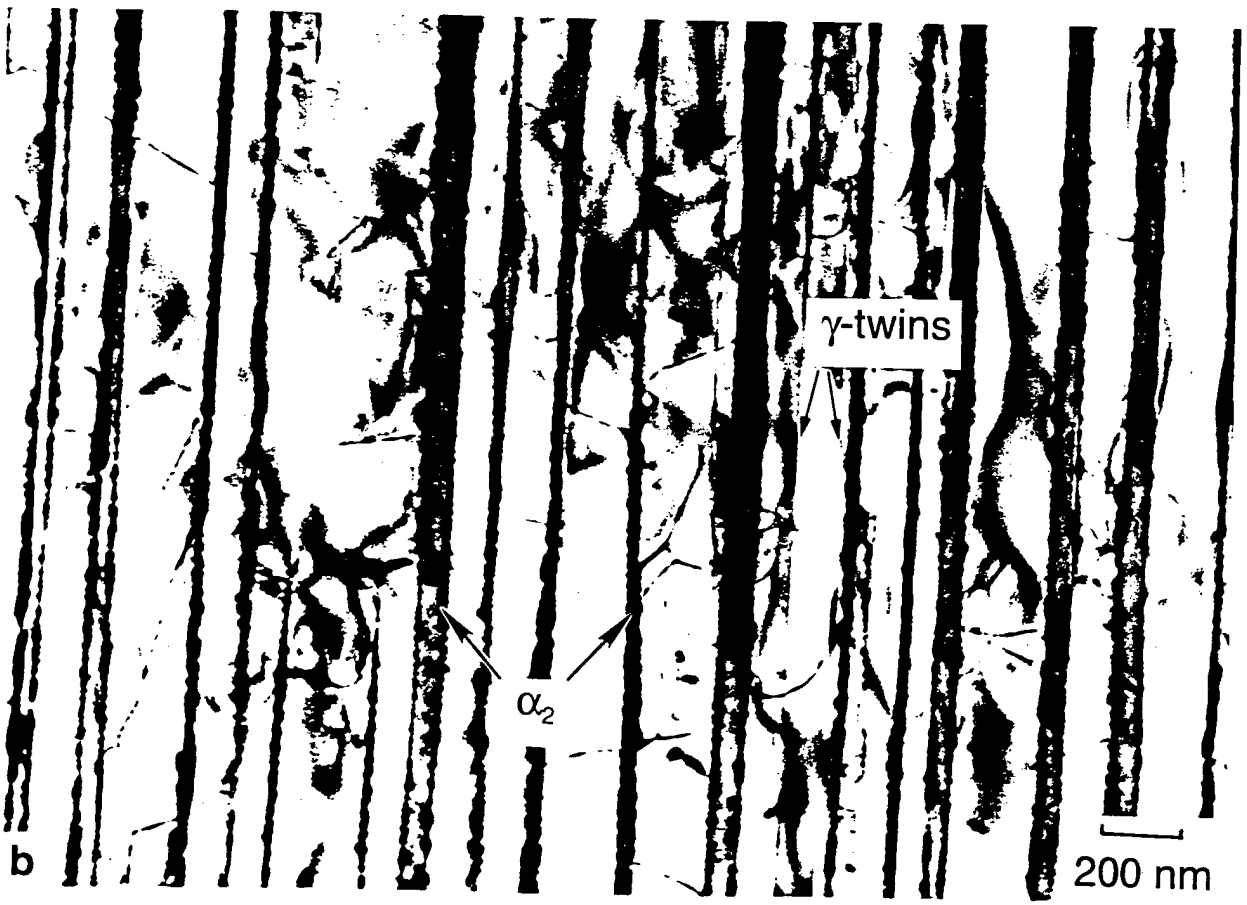

Fig. 2

SAD for DF images of phase constituents

Z = $<1120>\alpha_2$ x

$<101>\gamma$ ○

$<110>\gamma$ ●

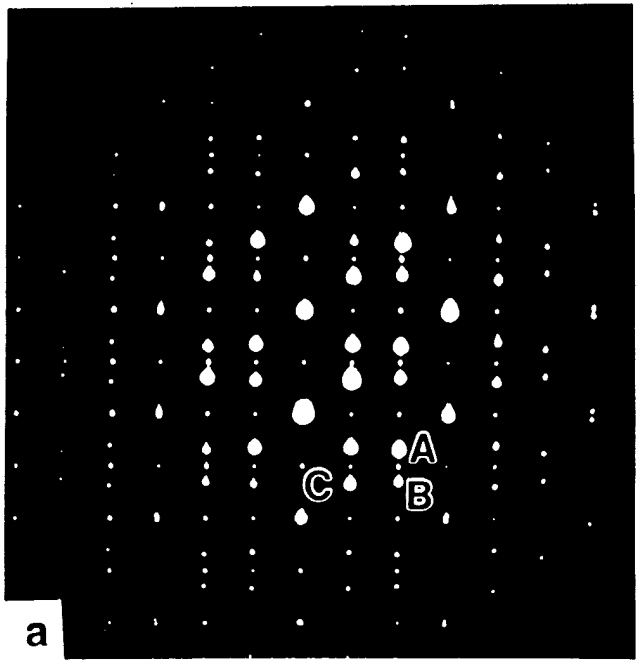

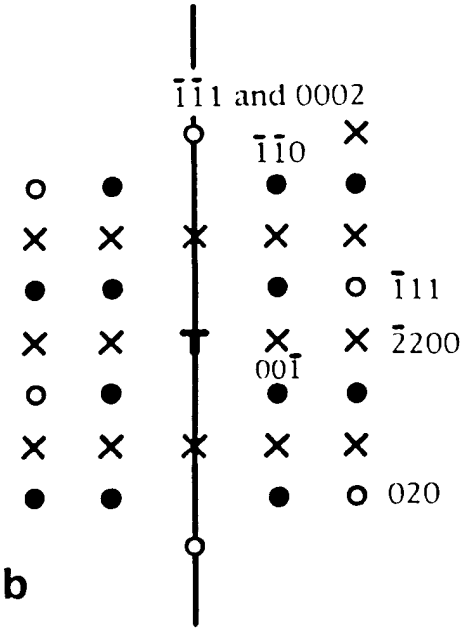

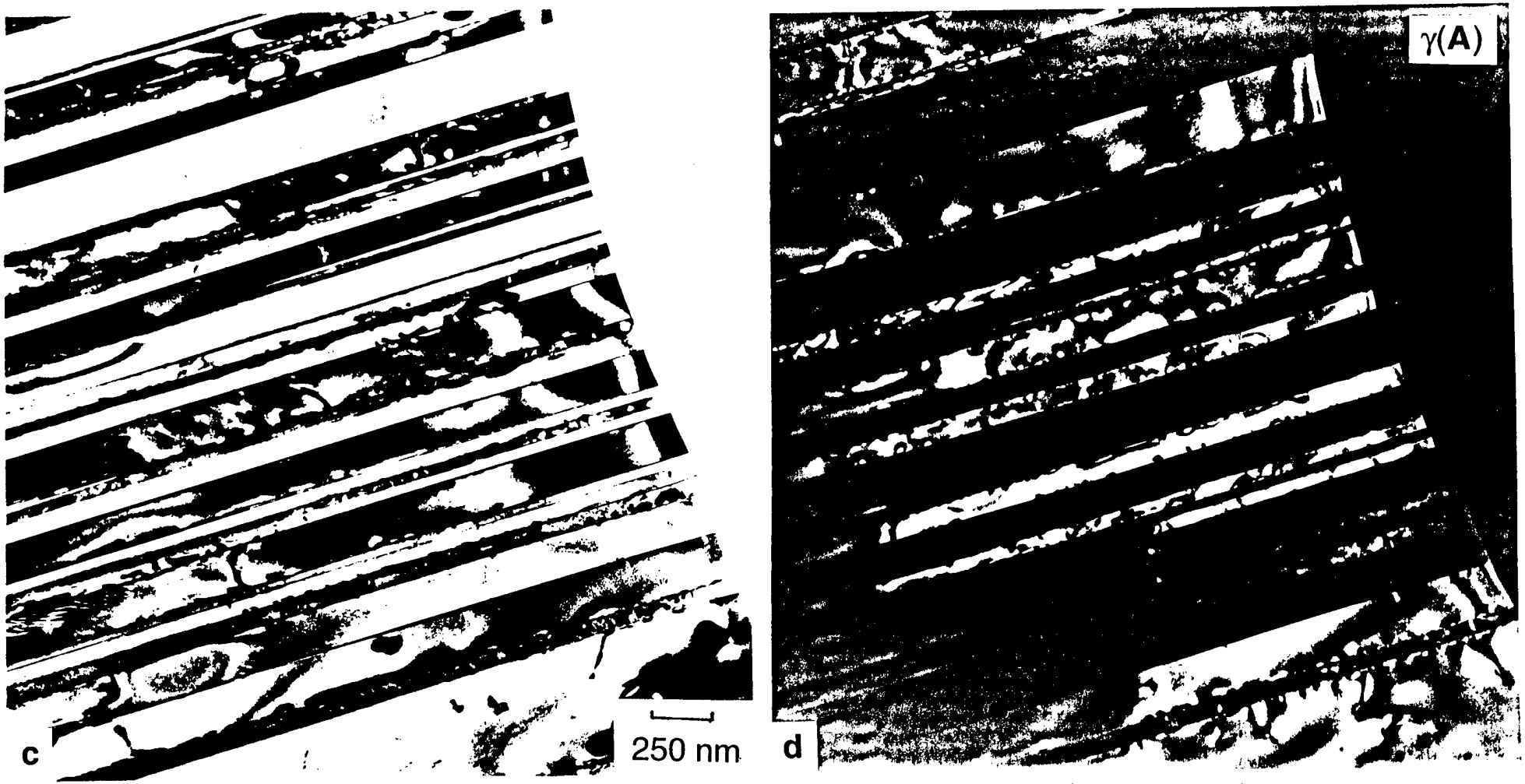
c
250 nm
d
γ(A)

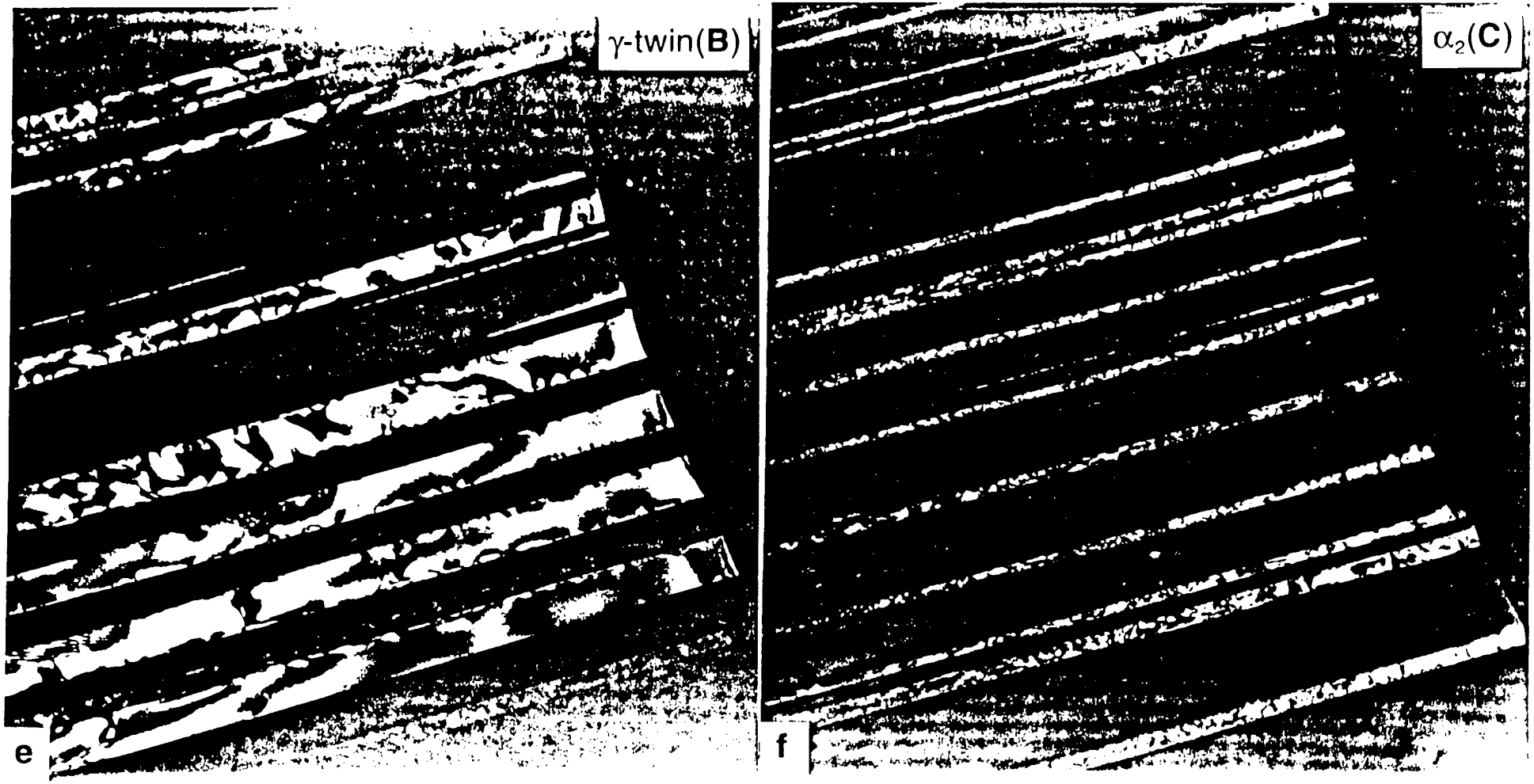
γ-twin(B)
e
α_2(C)
f

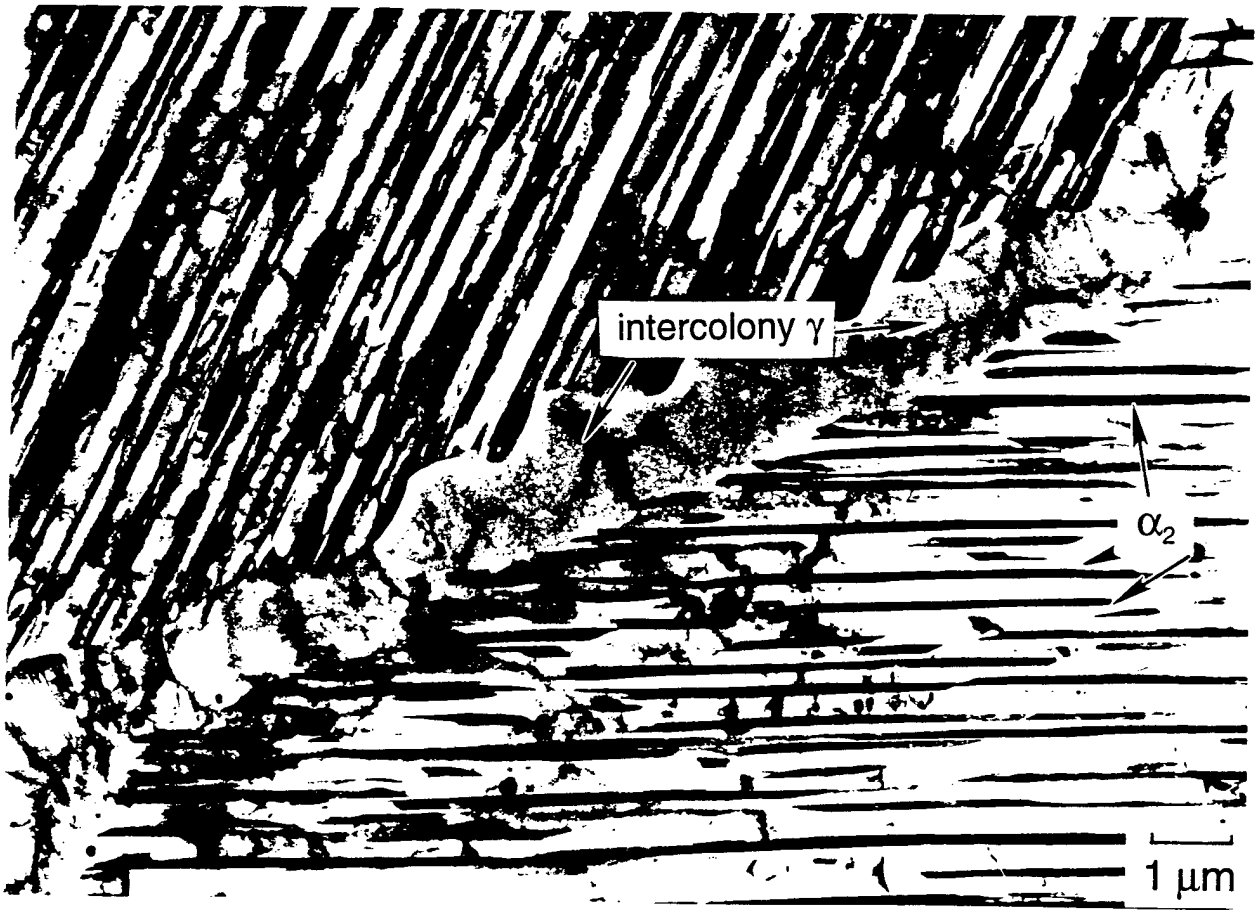

Fig. 4

2h at 1320°C

2h at 1350°C

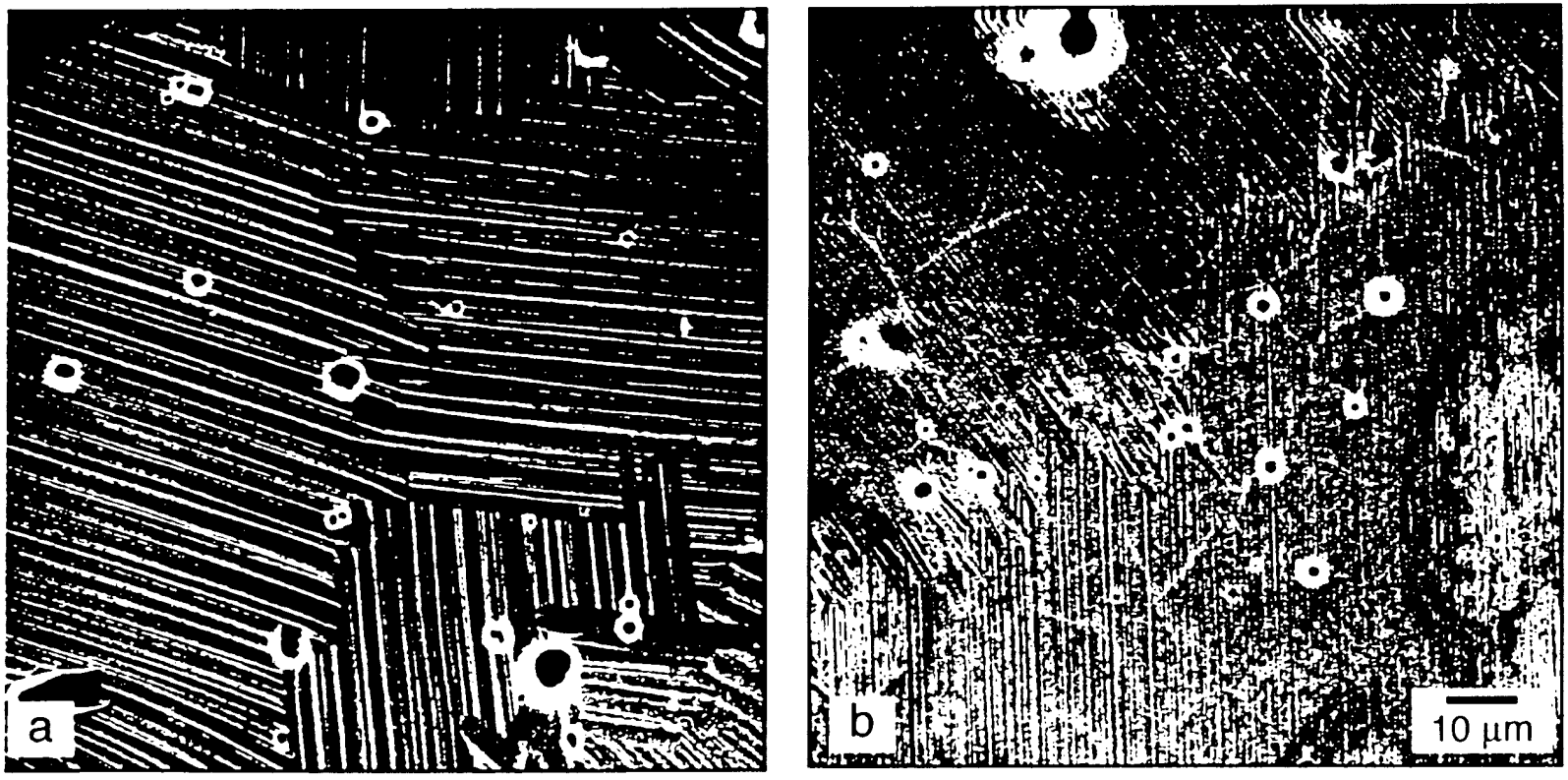

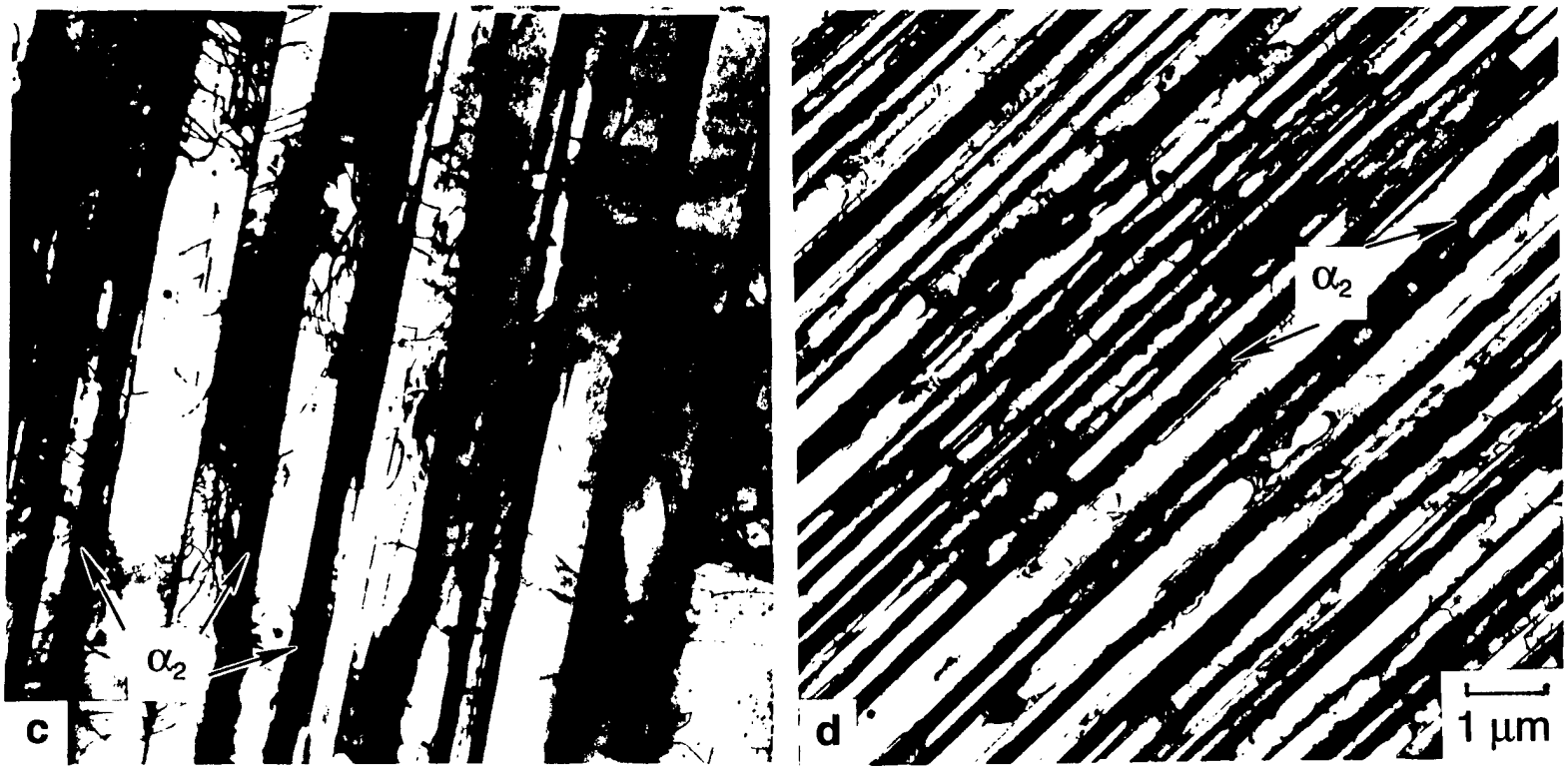
c
α_2
d
α_2
1 µm

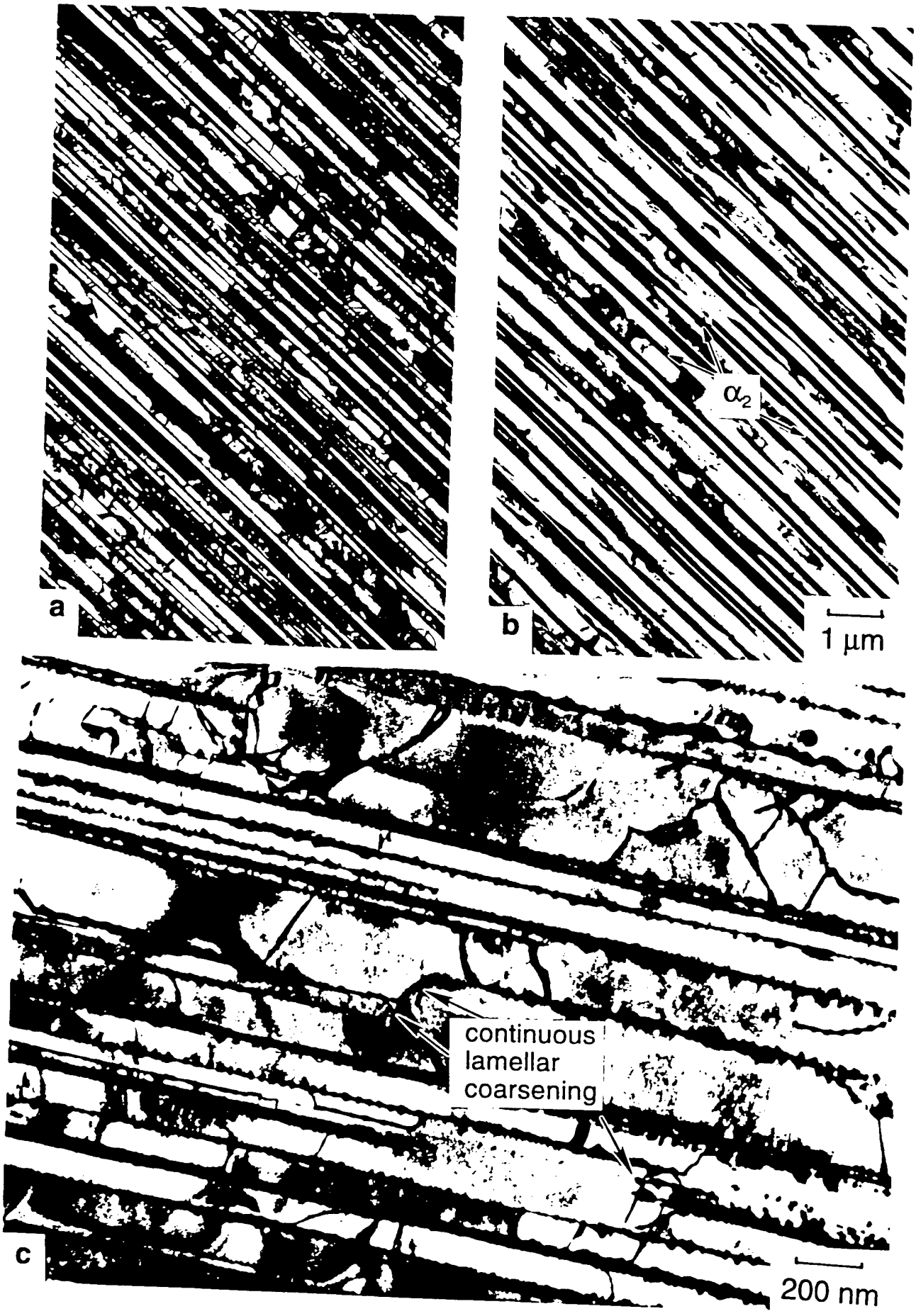

Fig. 6

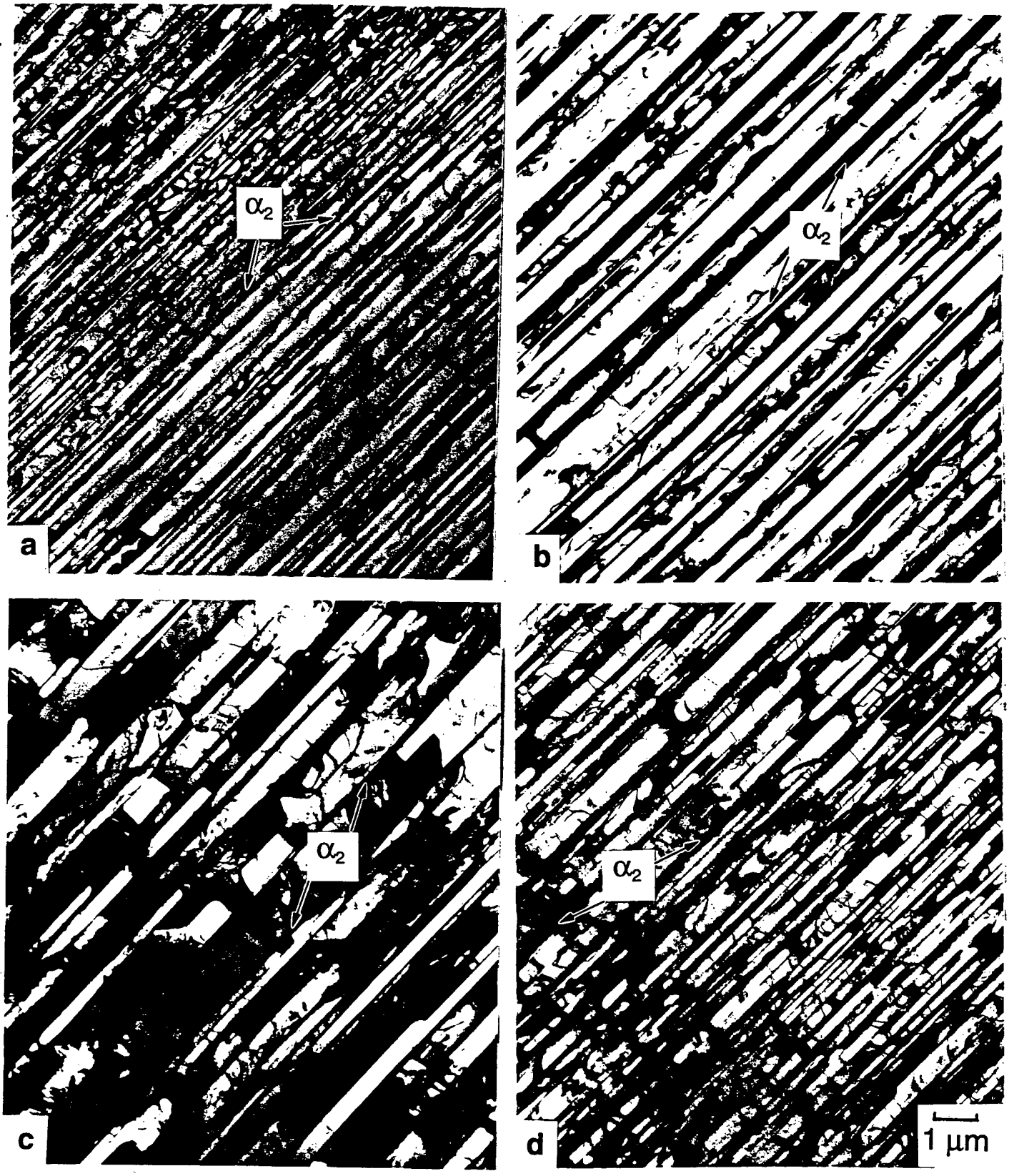

Fig. 7

Fig. 8

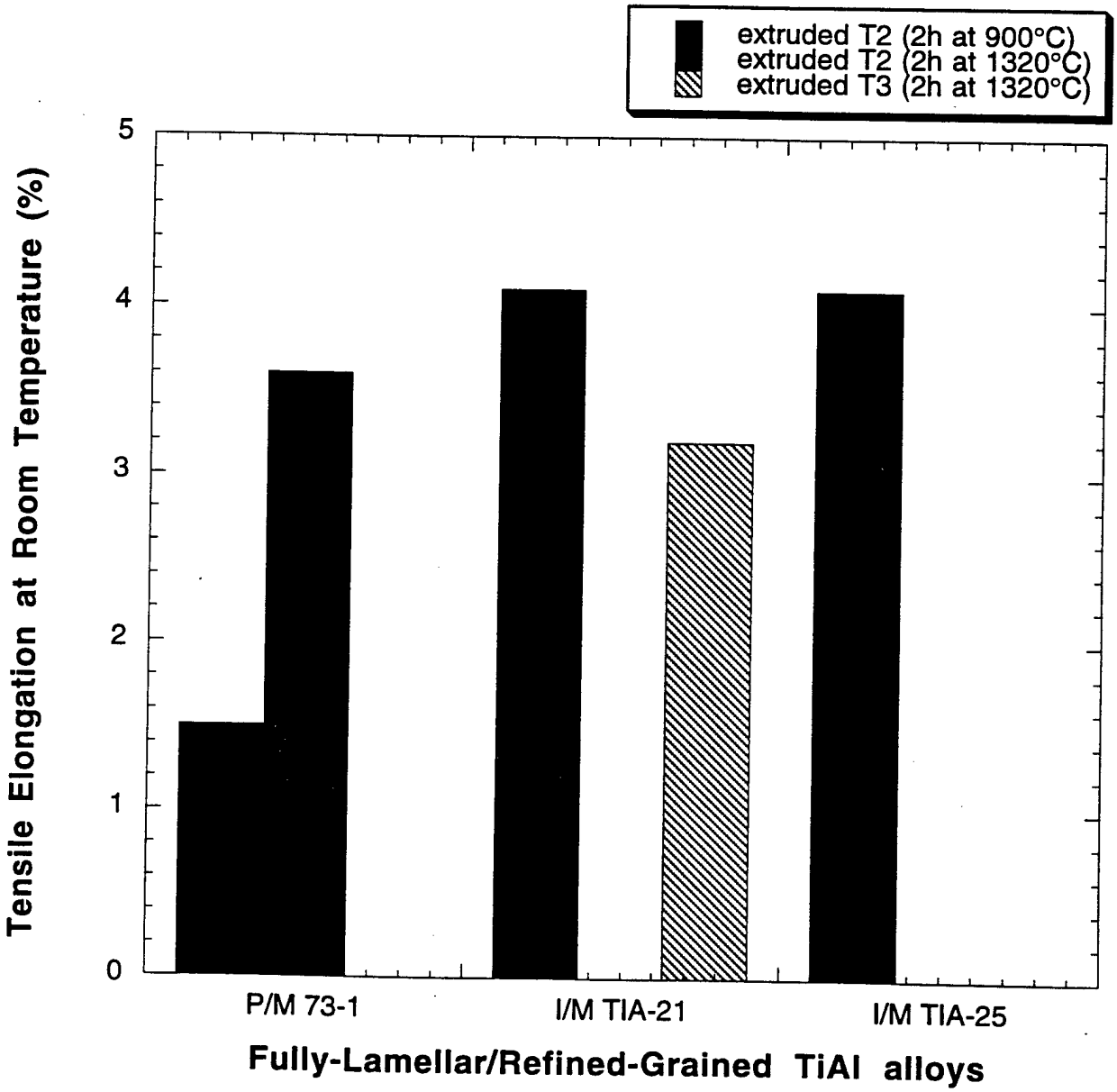
extruded T2 (2h at 900°C)
extruded T2 (2h at 1320°C)
extruded T3 (2h at 1320°C)
Tensile Elongation at Room Temperature (%)
0
1
2
3
4
5
P/M 73-1
I/M TIA-21
I/M TIA-25
Fully-Lamellar/Refined-Grained TiAl alloys

Fig. 9

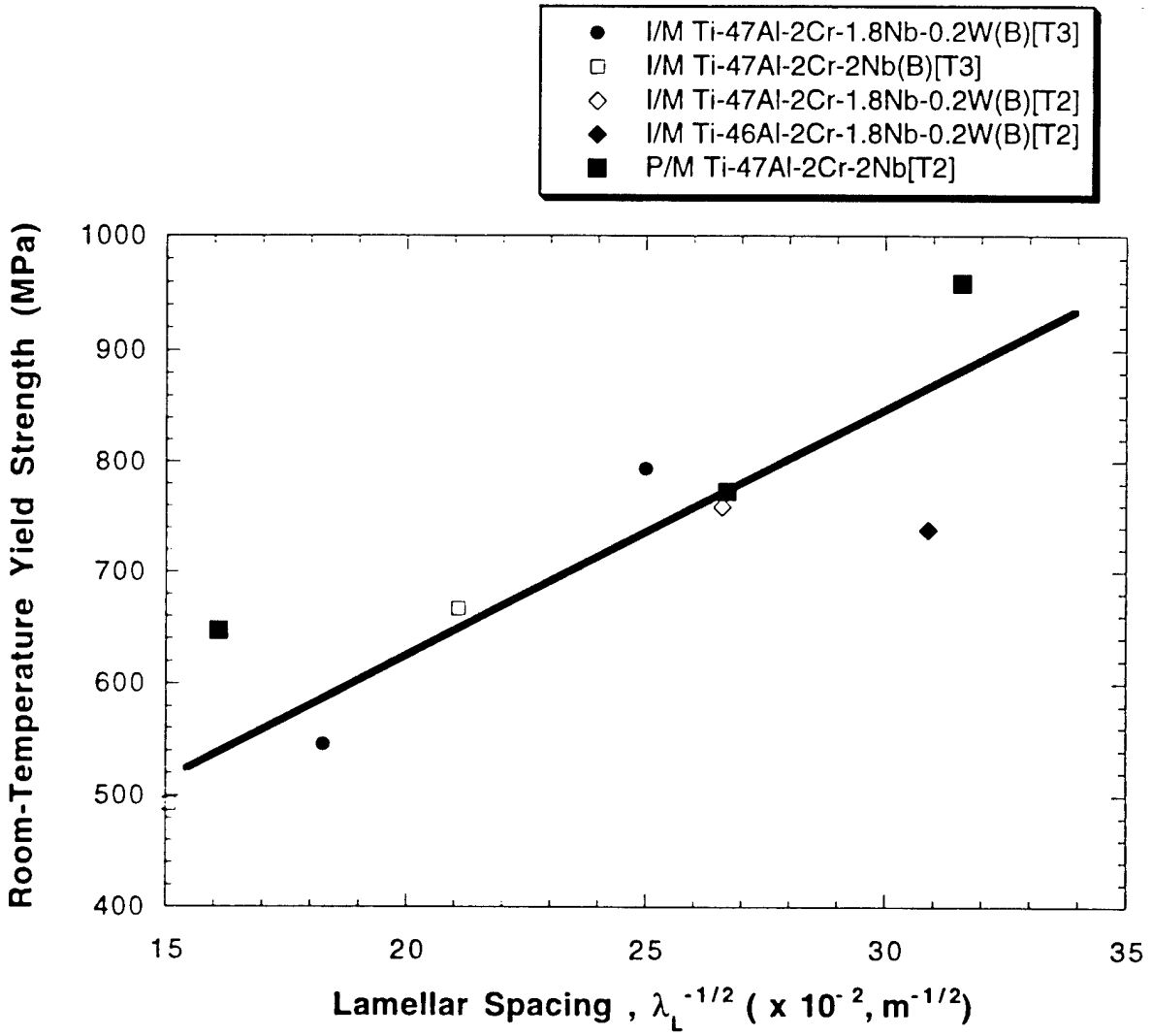
I/M Ti-47Al-2Cr-1.8Nb-0.2W(B)[T3]
I/M Ti-47Al-2Cr-2Nb(B)[T3]
I/M Ti-47Al-2Cr-1.8Nb-0.2W(B)[T2]
I/M Ti-46Al-2Cr-1.8Nb-0.2W(B)[T2]
P/M Ti-47Al-2Cr-2Nb[T2]
Room-Temperature Yield Strength (MPa)
1000
900
800
700
600
500
400
15
20
25
30
35
Lamellar Spacing , $\lambda_L^{-1/2}$ (x 10^{-2}, $m^{-1/2}$)

Fig. 10.

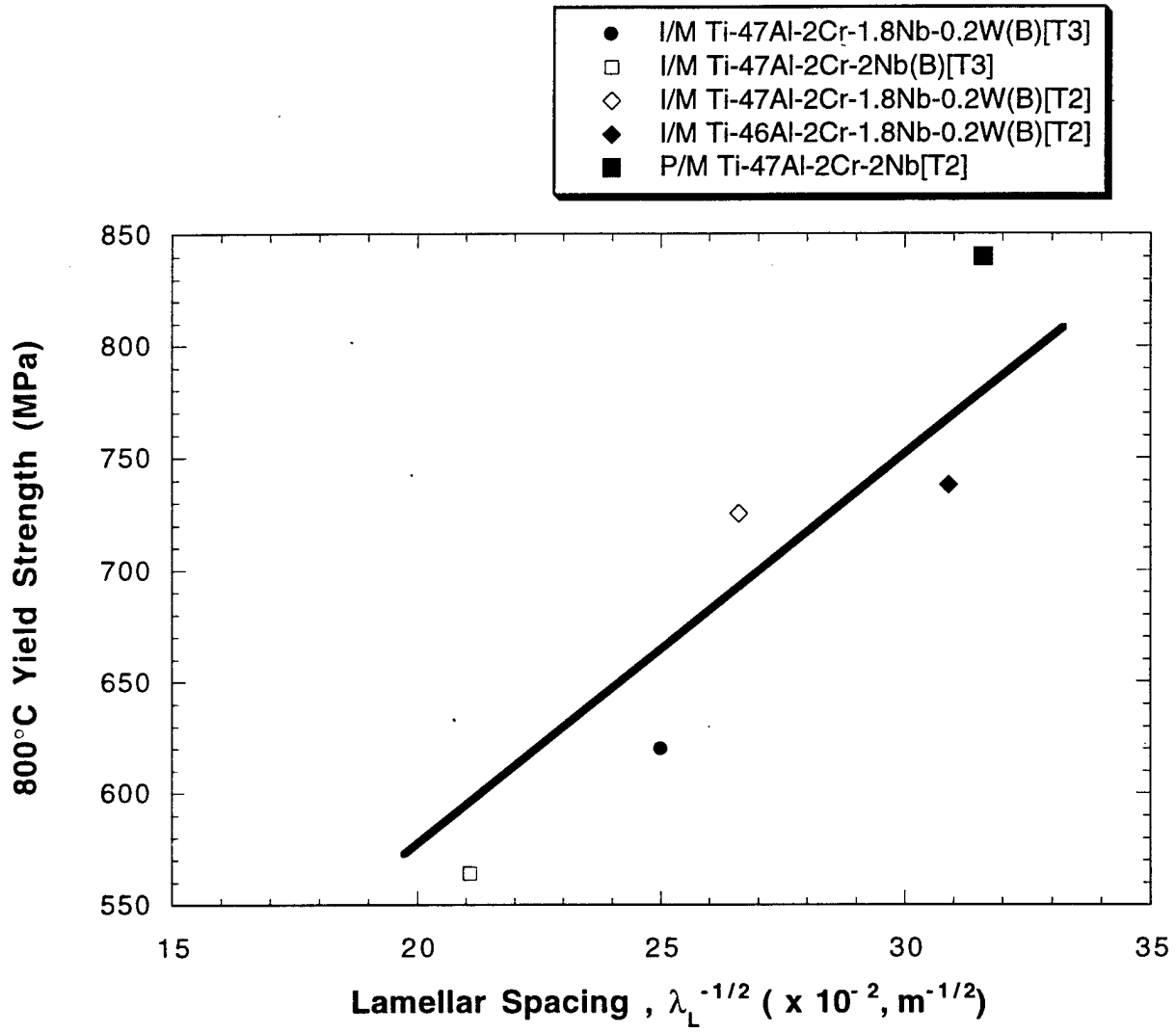
I/M Ti-47Al-2Cr-1.8Nb-0.2W(B)[T3]
I/M Ti-47Al-2Cr-2Nb(B)[T3]
I/M Ti-47Al-2Cr-1.8Nb-0.2W(B)[T2]
I/M Ti-46Al-2Cr-1.8Nb-0.2W(B)[T2]
P/M Ti-47Al-2Cr-2Nb[T2]
800°C Yield Strength (MPa)
850
800
750
700
650
600
550
15
20
25
30
35
Lamellar Spacing , $\lambda_L^{-1/2}$ (x 10^{-2}, $m^{-1/2}$)

Fig. 11

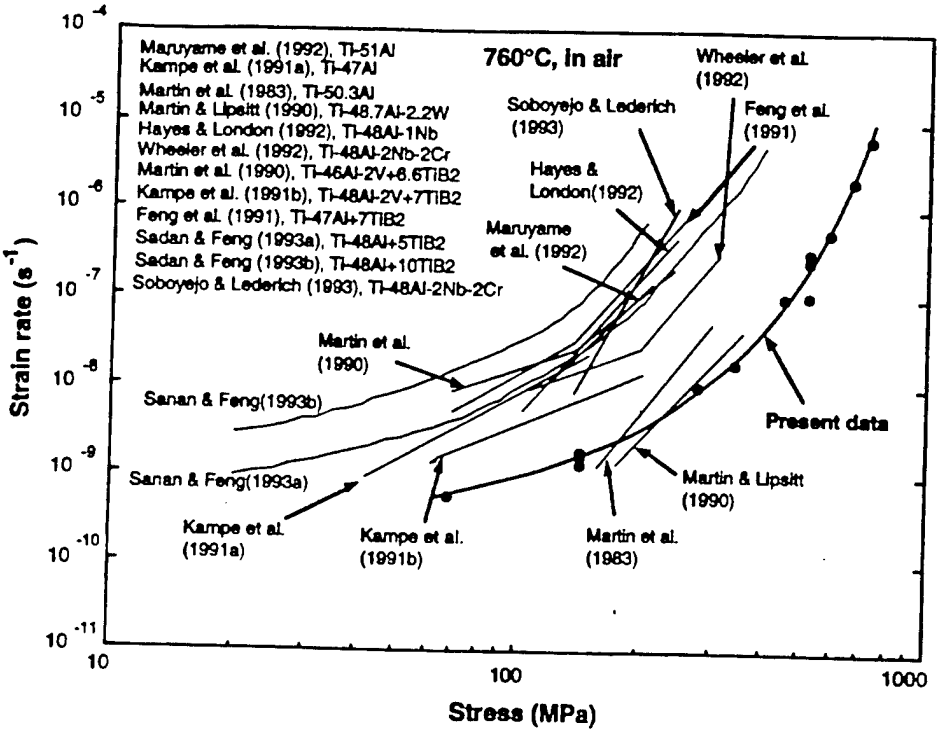
Maruyama et al. (1992), Ti-51Al
Kampe et al. (1991a), Ti-47Al
Martin et al. (1983), Ti-50.3Al
Martin & Lipsitt (1990), Ti-48.7Al-2.2W
Hayes & London (1992), Ti-48Al-1Nb
Wheeler et al. (1992), Ti-48Al-2Nb-2Cr
Martin et al. (1990), Ti-46Al-2V+6.6TiB2
Kampe et al. (1991b), Ti-48Al-2V+7TiB2
Feng et al. (1991), Ti-47Al+7TiB2
Sadan & Feng (1993a), Ti-48Al+5TiB2
Sadan & Feng (1993b), Ti-48Al+10TiB2
Soboyejo & Lederich (1993), Ti-48Al-2Nb-2Cr
760°C, in air
Wheeler et al. (1992)
Soboyejo & Lederich (1993)
Feng et al. (1991)
Hayes & London(1992)
Maruyama et al. (1992)
Martin et al. (1990)
Sanan & Feng(1993b)
Present data
Sanan & Feng(1993a)
Martin & Lipsitt (1990)
Kampe et al. (1991a)
Kampe et al. (1991b)
Martin et al. (1983)
Strain rate (s-1)
Stress (MPa)
10-4
10-5
10-6
10-7
10-8
10-9
10-10
10-11
10
100
1000

Fig. 12

DOE

(18) DOE, XF
(19) UC-900, DOE